INSTITUTE OF PHYSICS PUBLISHING JOURNAL OF PHYSICS B: ATOMIC, MOLECULAR AND OPTICAL PHYSICS

J. Phys. B: At. Mol. Opt. Phys. **38** (2005) 4389–4398 doi:10.1088/0953-4075/38/24/005

Vortices in two-component Bose–Einstein condensates

D M Jezek[1,2] **and P Capuzzi**[1,3]

[1] Departamento de Física, Facultad de Ciencias Exactas y Naturales, Universidad de Buenos Aires, RA-1428 Buenos Aires, Argentina
[2] Consejo Nacional de Investigaciones Científicas y Técnicas, Argentina
[3] NEST-INFM and Classe di Scienze, Scuola Normale Superiore, Piazza dei Cavalieri 7, I-56126 Pisa, Italy

E-mail: djezek@df.uba.ar and capuzzi@sns.it

Received 9 August 2005
Published 30 November 2005
Online at stacks.iop.org/JPhysB/38/4389

Abstract

We study the spatial distribution of particles in two-component Bose–Einstein condensates containing vortices. We show that the form in which the species are arranged inside the condensate may be easily understood using simple approximations. We obtain expressions for the location of particular points which are useful for describing the density of particles in two limiting situations, using either the Thomas–Fermi approximation or a low-dilution approximation. A discussion about the shape of vortex cores is also included.

1. Introduction

In the past few years, much experimental and theoretical work on Bose–Einstein condensation has dealt with vortices within systems comprising a mixture of two distinct species of atoms. One mixture commonly used is that of atoms of ^{87}Rb in two different hyperfine states $|F = 1, m_f = -1\rangle$ and $|F = 2, m_f = 1\rangle$. Experimentally, these mixtures are under such conditions that the two species may be considered as 'effectively distinguishable', and their mutual repulsion has been observed to lead to partial separation of both species in space [1].

From an experimental point of view, vortices have first been created in a mixture of these species of rubidium by Matthews *et al* [2]. The vortex was created in either of the two components, through a coherent process involving the spatial and temporal control of interconversion between the two components. Later, using the same techniques, Anderson *et al* [3] created off-centred vortices and studied their preceding dynamics around a definite axis. Also using these mixtures, vortex rings were obtained as a result of the decay of dark solitons [4]. Recently, in a very nice experiment, Schweikhard *et al* [5] observed interlaced square vortex lattices in a rotating system as a consequence of separation effects between species.

On the other hand, from a theoretical point of view, much work has been devoted to describe these systems. As the number of particles involved in experiments is large, almost

all the theory has been based on the Thomas–Fermi (TF) approximation. In this sense, in a pioneering paper, Ho and Shenoy [6] have constructed an elegant algorithm to determine the TF density profiles of binary mixtures which may include vortices. In a previous work, we have presented a simpler procedure [7] to obtain the wavefunctions in the same approximation. An advantage of our method is that one can directly find analytic expressions for the densities and hence extract much geometrical information related to the distribution of species in space, without performing any numerical calculation. In particular, in [7] we showed that it is possible to study the distribution of particles by classifying the interface between the species in two families of surfaces, depending on which component carries the vorticity. The problem of vortices in phase-separated two-component systems has also been addressed in the TF approximation by Chui *et al* in [8–10]. In these papers, the authors assumed that the vortices have cores with radii of the same order of magnitude as those of a vortex in a single-component condensate. Recently, Park and Eberly [11] have studied a class of non-topological vortices in two-component Bose–Einstein condensate assuming an $SU(2)$ symmetry. They used this symmetry to describe a system of rubidium atoms, based on the fact that both species have very similar scattering lengths.

In the present paper, we focus on the study of the spatial structure of vortices in two-component condensates. Our study also includes the analysis of the redistribution of particles inside the trap when one of the species is loaded in a shifted confining potential. We derive analytic expressions for the density profiles in two limiting situations using either the TF approximation or a low-dilution approximation and compare these results with the solutions of the exact Gross–Pitaevskii (GP) equations. Some of the properties we have encountered are as follows. Firstly, for a mixture the vortex-core size may be much larger than the healing length, as it has been observed experimentally [3]. Secondly, although the scattering lengths are very similar for both species, we have observed qualitatively different features with respect to interchanging the type of particles. And finally, for systems confined in slightly shifted potentials, we show that in a small range of values of interparticle coupling the distribution of species undergoes dramatic changes. A similar behaviour has also been encountered for vortex-free systems in [12, 13].

The paper is organized as follows. Section 2 describes in detail the physical system under study. In section 3 we analyse the spatial distribution of species in two limiting cases, (i) when the number of particles of both species is large enough to rely on the Thomas–Fermi approximation, and (ii) when the number of particles of one species is much smaller than the other. The numerical solutions of the full Gross–Pitaevskii (GP) equations are presented in section 4. In order to clarify some ideas, in this section we also give some results for two-dimensional systems. Finally, section 5 contains the summary and main conclusions of our work.

2. The system

We consider a dilute mixture of two hyperfine species of the same bosonic atoms confined in axially symmetric harmonic traps. The confinement of one species, arbitrarily chosen to be the species 2, is displaced in the z-direction in a value $-d$. The confining potentials can then be written as

$$V_1(\boldsymbol{r}) = \tfrac{1}{2}M\left(\omega_r^2 r^2 + \omega_z^2 z^2\right) \tag{1}$$

and

$$V_2(\boldsymbol{r}) = \tfrac{1}{2}M\left(\omega_r^2 r^2 + \omega_z^2 (z+d)^2\right), \tag{2}$$

where M is the mass of the atoms, and ω_r and ω_z denote the angular trapping frequencies.

In order to describe the ground state of the mixture at zero temperature, we resort to the coupled Gross–Pitaevskii equations for the wavefunctions ψ_i [14] of each species i,

$$\left(-\frac{\hbar^2\nabla^2}{2M} + V_i(\boldsymbol{r}) + \sum_{k=1,2} N_k G_{ik}|\psi_k|^2\right)\psi_i = \mu_i\psi_i, \tag{3}$$

where N_i denotes the number of atoms of species i, μ_i is the chemical potential and we have the normalization condition $\int |\psi_i|^2\,\mathrm{d}\boldsymbol{r} = 1$. The coupling strengths can be written in terms of the s-wave scattering lengths a_{kl} between species k and l as $G_{kl} = 4\pi a_{kl}\hbar^2/M$.

For simplicity, we fix the most repulsive component in the state ψ_1 and factorize the coupling strengths as $G_{kl} = u_{kl}U$, with $U = 4\pi\hbar^2 a_{11}/M$, and thus $u_{11} = 1\,(> u_{22})$. In the numerical calculations, we will consider a mixture of ^{87}Rb atoms with relative scattering lengths $u_{12} = 0.97$ and $u_{22} = 0.94$ [15] and restrict ourselves to spherical traps with angular frequency $\omega_r = \omega_z = 2\pi\nu_{\mathrm{trap}}$, where $\nu_{\mathrm{trap}} = 7.8$ Hz.

3. Limiting cases

3.1. Thomas–Fermi regime

When both components have a considerable number of particles, the well-known TF approximation provides reliable results for the density profiles. For vortex-free structures, this approach ignores all the kinetic energy contained in the $\nabla^2\psi_i$ terms in (3). However, if the species j possesses a vortex its wavefunction reads $\psi_j(\boldsymbol{r}) = \psi_j(r, z)\,\mathrm{e}^{\mathrm{i}m_j\phi}$, where ϕ is the polar angle and m_j its vorticity. In this case, the TF approximation amounts to retaining only the centrifugal term derived from the angular derivatives of the Laplacian giving rise to an effective potential $V_i^{\mathrm{eff}}(\boldsymbol{r})$.

Hereafter, we shall use the oscillator length $d_{\mathrm{ho}} = \sqrt{\hbar/M\omega_z}$ as a unit of length and $\hbar\omega_z/2$ as a unit of energy. In these units, the effective potentials read

$$V_1^{\mathrm{eff}}(\boldsymbol{r}) = \lambda^2 r^2 + z^2 + \frac{\kappa_1}{r^2} \tag{4}$$

and

$$V_2^{\mathrm{eff}}(\boldsymbol{r}) = \lambda^2 r^2 + (z+d)^2 + \frac{\kappa_2}{r^2}, \tag{5}$$

where $\kappa_i = m_i^2/4$ is the rescaled vorticity and $\lambda = \omega_r/\omega_z$ is the aspect ratio of the trap.

The sign of $\Delta \equiv u_{11}u_{22} - u_{12}^2$ defines two different ways in which the distribution of particles may occur. When $\Delta > 0$ the two components coexist in some region of space. As u_{12} increases this region decreases until at $\Delta = 0$ a spatial phase separation takes place, reducing the coexistence region to an interface. We shall consider these two cases separately.

Coexistence $\Delta > 0$. The solution of (3) in the TF approximation can be easily obtained and has the following expressions depending on whether there exists any overlap between the species:

(a) In the regions where only one wavefunction is non-vanishing ($|\psi_i|^2 \neq 0$ and $|\psi_k|^2 = 0$, for $i \neq k$). The TF equations are decoupled and the solutions read

$$\begin{aligned} |\psi_1|^2 &= \left[\mu_1 - \lambda^2 r^2 - z^2 - \frac{\kappa_1}{r^2}\right] \Big/ (G_{11}N_1) \\ |\psi_2|^2 &= \left[\mu_2 - \lambda^2 r^2 - (z+d)^2 - \frac{\kappa_2}{r^2}\right] \Big/ (G_{22}N_2). \end{aligned} \tag{6}$$

The boundary of each condensate is obtained by equating the expressions inside the square brackets to zero. For species 1 the boundary surface is centred at $(x, y, z) = (0, 0, 0)$, while for species 2 it is centred at $(x, y, z) = (0, 0, -d)$.

(b) In the region where both wavefunctions are non-vanishing the solution can be written after some algebra as

$$
\begin{aligned}
|\psi_1|^2 &= \left[C_1^2 - \lambda^2 r^2 - \left(z - \frac{\beta_1 d}{1-\beta_1} \right)^2 + \frac{\kappa_2 \beta_1 - \kappa_1}{(1-\beta_1) r^2} \right] B_1 u_{22} \\
|\psi_2|^2 &= \left[C_2^2 - \lambda^2 r^2 - \left(z + \frac{d}{1-\beta_2} \right)^2 + \frac{\kappa_1 \beta_2 - \kappa_2}{(1-\beta_2) r^2} \right] B_2 u_{11},
\end{aligned}
\tag{7}
$$

where

$$
C_i^2 = \frac{\mu_i - \beta_i \mu_j}{(1-\beta_i)} + \frac{\beta_i d^2}{(1-\beta_i)^2} \qquad \text{for} \quad i, j = 1, 2 \quad \text{and} \quad j \neq i, \tag{8}
$$

$\beta_1 = u_{12}/u_{22}$, $\beta_2 = u_{12}/u_{11}$, and $B_i = (1-\beta_i)/(U N_i \Delta)$.

The coexistence region is delimited by two surfaces, $\mathcal{S}_1$ and $\mathcal{S}_2$, defined by equating to zero the expression inside the square brackets in $|\psi_1|^2$ and $|\psi_2|^2$ of (7). These surfaces may be classified as done in [7], with the only difference that in the present case they are shifted in the z-direction. In addition, they are axially symmetric around the z-axis and possess an inversion symmetry with respect to the point $(x, y, z) = (0, 0, d_i)$ with $i = 1, 2$, and d_i given by $d_1 = \beta_1 d/(1-\beta_1)$ and $d_2 = -d/(1-\beta_2)$, respectively. The factor $1 - \beta_i$ in the denominator makes these displacements diverge when β_i is close to unity, and one can guess that, depending on the relative magnitude between the interaction strengths, some dramatic effects in the redistribution of particles should take place. In a previous work [12] we have already discussed this effect and showed that it is consistent with the experimental data of [15].

It is worthwhile mentioning that although much information can be read directly from the form of (6) and (7), to obtain the full wavefunctions one needs the values of C_i and hence the chemical potentials. This has to be done numerically using the fact that the wavefunctions have to be normalized to one.

Phase separation $\Delta \leqslant 0$. When the intercomponent repulsion overcomes the repulsion inside each species, the two species demix, i.e, segregate into two non-overlapping regions in space. As we have already mentioned, in the TF approximation this transition occurs at $\Delta = 0$. The limiting surface ($\mathcal{S}_s$) between these non-overlapping regions can be obtained by imposing its mechanical equilibrium. This is achieved by equating the pressure [14]

$$
P_i = \frac{G_{ii}}{2} \rho_i^2 = \frac{G_{ii}}{2} N_i^2 |\psi_i|^4 \tag{9}
$$

on both sides of the interface, which yields the condition

$$
N_1 |\psi_1|^2 = \sqrt{\frac{G_{22}}{G_{11}}} N_2 |\psi_2|^2. \tag{10}
$$

Assuming that the wavefunctions on each side are given by (6) and defining $a = \sqrt{G_{22}/G_{11}}$, (10) can be rewritten as

$$
C_s^2 - \lambda^2 r^2 - \left(z + \frac{d}{1-a} \right)^2 + \frac{\kappa_1 a - \kappa_2}{(1-a) r^2} = 0 \tag{11}
$$

where

$$
C_s^2 = \frac{\mu_2 - a \mu_1}{(1-a)} + \frac{a d^2}{(1-a)^2}. \tag{12}
$$

The interface is thus displaced in the z-direction in a value $d_s = -d/(1-a)$. Note that for the ^{87}Rb species of [15], the values of the interaction strengths give a small and negative Δ value, $\Delta \simeq -9 \times 10^{-4}$, and an a close to unity, $a = 0.969$. As a consequence, the absolute value of d_s is increased with respect to the initial displacement of the potentials by a factor of 32.8. For example, if we have a distance between the trap centres $d = 0.2\,\mu$m, d_s turns out to be $d_s = -6.56\,\mu$m.

Another interesting point to discuss is the size of the vortex cores. The last term in (11) is responsible for their enlargement. Once more we see that the ratio between the scattering lengths has an important role. We shall come back to this discussion in section 4 where the analysis will not be restricted to this approximation.

3.2. Low-dilution regime

Let us next consider a condensate formed by a large number of particles N_1. We make a simplification by taking into account a few particles of species 2 immersed in the 1-species condensate and confined in the shifted potential V_2. If the component 2 has a vortex, the total effective potential experienced by these particles can be written as

$$V_2^{\mathrm{e}}(\boldsymbol{r}) = \lambda^2 r^2 + \frac{\kappa_2}{r^2} + (z+d)^2 + G_{12}\rho_1, \tag{13}$$

where ρ_1 is the *uncoupled* density of species 1. In the TF approximation, it reads

$$\rho_1(\boldsymbol{r}) = \frac{1}{G_{11}}(\mu_1 - \lambda^2 r^2 - z^2)\Theta(\mu_1 - \lambda^2 r^2 - z^2), \tag{14}$$

where Θ is the Heaviside function.

Replacing ρ_1 into (13) and defining $p_2 = 1 - \beta_2$, we find that V_2^{e} is approximately given by

$$V_2^{\mathrm{e}} \simeq \lambda^2 p_2 r^2 + \frac{\kappa_2}{r^2} + p_2\left(z + \frac{d}{p_2}\right)^2 - \frac{d^2}{p_2} + d^2 + \frac{u_{12}}{u_{11}}\mu_1, \tag{15}$$

which is valid inside the condensate.

The minimum of V_2^{e} is attained over a circle with cylindrical coordinates

$$r' = [\kappa_2/(p_2\lambda^2)]^{1/4} \qquad \text{and} \qquad z' = -d/p_2. \tag{16}$$

The N_2 particles will be mainly distributed along this circle forming an annular vortex. This ring is not centred at the minimum of the bare trap V_2 potential, but it is displaced in a distance $|z'|$ which may be quite different from the original trap displacement. For example, using the values of the scattering lengths of the rubidium mixture we obtain $1/p_2 \sim 33.3$, and thus $|z'|$ is about 33 times larger than d. Regarding the shape of the density profile, in figure 1 we plot the effective potential $V_2^{\mathrm{e}}(r)$ at $z = 0$ for $d = 0$ and $N_1 = 10^7$ obtained using the GP density profile for $\rho_1(\boldsymbol{r})$. In figure 1 we also show the density profile ρ_2 for $N_2 = 10^3$. From top to bottom the curves correspond to the values $z = 0, 5, 10, 15$ and $20\,\mu$m. The vertical dotted line locates the radius $r' = 9.25\ \mu$m according to (16). This radius may be increased by decreasing the radial frequency since r' turns out to be proportional to $\omega_r^{-1/2}$.

Let us now consider the opposite dilute regime where few particles of the species 1 interact with a large condensate of N_2 particles. The new distribution of the species can be analysed by interchanging the indexes 1 and 2 in the previous formulae. We then find $p_1 < 0$ and hence the effective potential V_1^{e} turns out to be a monotonously decreasing function of r as long as ρ_2 is non-vanishing. This implies that there is no circle analogous to that defined in (16). In this case, the species 1 is located at the border of the condensate where ρ_2 goes to zero and the actual minimum of V_1^{e} is reached. In figure 2 we show V_1^{e} as a function of r for $z = 0$.

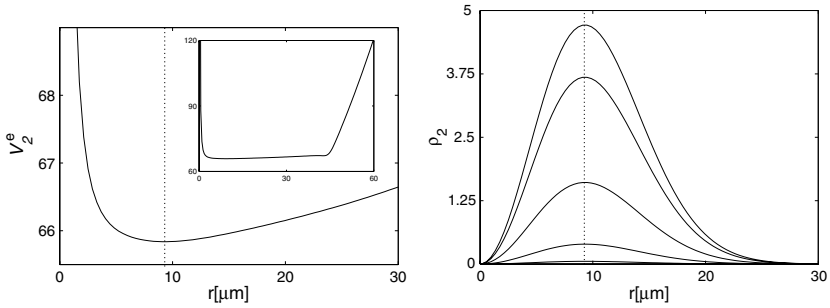

Figure 1. Low-dilution regime of a mixture of ^{87}Rb atoms with $N_1 = 10^7$ and a vortex in the state $|2\rangle$. Left panel: effective potential V_2^e (in arbitrary units) as a function of r (in μm) at $z = 0$. The inset shows the confinement in a larger range. Right panel: density profile ρ_2 (in arbitrary units) as a function of r (in μm) at several values of $z = 0, 5, 10, 15$, and 20 μm from top to bottom curves. The vertical dotted lines indicate r' (see the text).

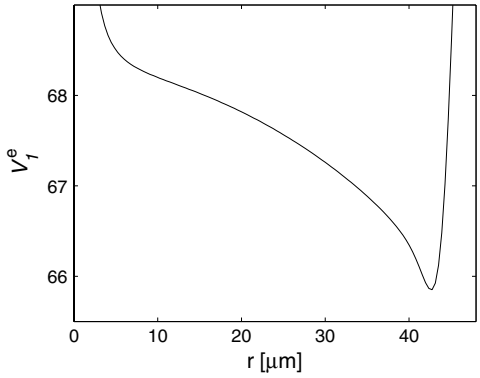

Figure 2. Effective potential V_1^e (in arbitrary units) as a function of r (in μm) for a mixture in the dilute regime with $N_2 = 10^7$ and $m_1 = 1$.

Note that here the derivative at the border of the condensate is continuous because we have calculated ρ_2 by solving the GP equations, and thus the behaviour of the function around the minimum is smoother than the one that is obtained using the TF approximation.

4. Full Gross–Pitaevskii solutions

In this section, we analyse the density profiles calculated by solving the exact GP equations and compare to the TF results of the previous section. In particular, we remind the reader that for this mixture the scattering lengths verify $\Delta \lesssim 0$, i.e., we are in the phase-separated regime.

The numerical solution of the coupled (3) is carried out in the standard way, using a steepest-descent method [16] to minimize the total GP energy functional for given numbers of particles. In particular, we have discretized the wavefunctions on a grid of 100×200 points in the rz plane and convergence of the self-consistent procedure was achieved with at least five figures of accuracy in the chemical potentials.

In order to compare the GP results with the TF solutions, we introduce the surfaces defined by

$$\alpha_1 \rho_1 - \alpha_2 \rho_2 = 0, \tag{17}$$

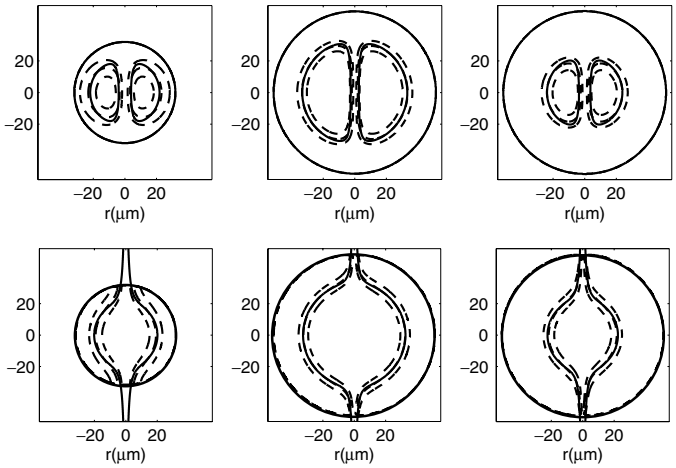

Figure 3. The density surfaces $S_>$, $S_<$ and S_e (dashed lines), together with the TF interface (solid line) for the first (second) row correspond to vorticity in component $|2\rangle$ ($|1\rangle$). The left, middle and right panels correspond to mixtures with $N_1 = N_2 = 10^6$, $N_1 = N_2 = 10^7$, and $N_1 = 1.6 \times 10^7$ and $N_2 = 4 \times 10^6$, respectively.

and consider three cases: (i) $\alpha_1 = \alpha_2 = 0.5$; (ii) $\alpha_1 = 0.2$ and $\alpha_2 = 0.8$; and (iii) $\alpha_1 = 0.8$ and $\alpha_2 = 0.2$. These values of α_i define the surfaces S_e, $S_>$ and $S_<$, respectively.

The surface S_e is expected to be located near to the TF interface given by (11), while the size of the region which remains between $S_>$ and $S_<$ can be taken as a measure of the accuracy of the TF approximation. The narrower this region is, the better the TF approximation works.

In the first (second) row of figure 3 we display these surfaces, together with the TF interface for $m_1 = 0$ and $m_2 = 1$ ($m_1 = 1$ and $m_2 = 0$), and $d = 0$. We consider three sets of numbers of particles: (i) $N_1 = N_2 = 1 \times 10^6$, (ii) $N_1 = N_2 = 1 \times 10^7$, and (iii) $N_1 = 1.6 \times 10^7$ and $N_2 = 4 \times 10^6$. We observe that the TF interface gives a good estimate of the S_e surface, although the GP densities are smoother functions than the TF ones. For $N_i = 10^6$ there exists a large overlapping region. It may be seen that the accuracy of the TF approximation is improved for an increasing number of particles. In particular, the distance between $S_>$ and $S_<$ is a monotonously decreasing function of N_i.

In figure 4 we display the same surfaces as those shown in figure 3 but with the V_2 potential displaced in a distance $d = 0.2\,\mu$m. Although this displacement is about 0.2% of the total size of the condensate, it may be seen that it sizably affects the distribution of particles, as it has been already predicted in the TF approximation. In particular, the TF interface mentioned in the previous section is centred at the z-value $d_s = -6.56\,\mu$m.

Let us now focus on the structure of the vortex cores. The density profile of one-component condensate in the TF limit is given by [17]

$$\rho = \rho_0 \left(1 - \frac{\xi^2}{r^2} - \frac{r^2}{R_c^2} - \frac{z^2}{Z_c^2}\right) \Theta \left(1 - \frac{\xi^2}{r^2} - \frac{r^2}{R_c^2} - \frac{z^2}{Z_c^2}\right), \tag{18}$$

where ξ is the so-called healing length [17], and R_c and Z_c are the radii of the condensate along r and z respectively. In this approximation the relation $\xi \ll R_c$ is verified. From (18) it is easy to prove that at $z = 0$ the TF density goes to zero when $r \sim \xi$. Thus for vortices in one-component systems the healing length is about the size of the vortex core. Chui *et al* [9] have taken this result as valid also in two-component condensates while it may be seen from the GPE results depicted in figures 3 and 4 that the cores are much larger. Moreover,

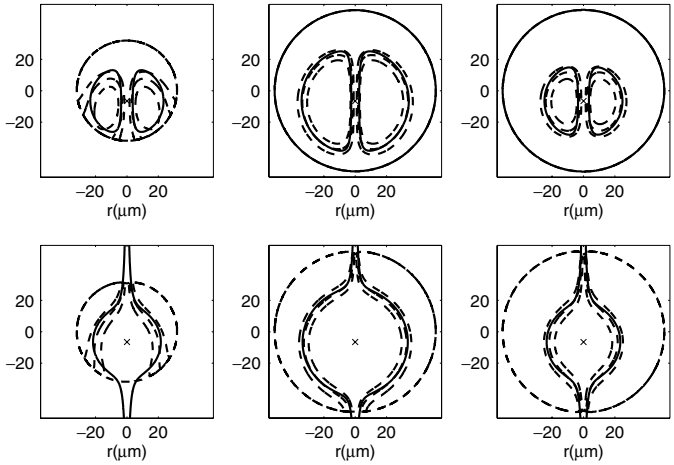

Figure 4. The same as figure 3 with a nonzero displacement $d = 0.2\,\mu$m. The crosses indicate the symmetry point of the TF interfaces, with coordinates $z = d_s = -6.56\,\mu$m and $r = 0$.

when the vortex is in component 1, its core is not homogeneous along the z-axis and thus it is hard to refer to a single vortex size, nevertheless for all z-values the size is visibly larger than the healing length. In contrast, a vortex in component 2 has an almost uniform core and its size, although smaller than that in the previous case, is still larger than the healing length, as we shall see. Quantitatively, for $N = N_1 + N_2 = 2 \times 10^6$ the healing length is $\xi = 0.45\,\mu$m while for $N = 2 \times 10^7$, $\xi = 0.28\,\mu$m. We have numerically calculated the radius at which the TF density goes to zero at $z = 0$ for the first row of figure 3. We obtained $r_1 = 3.9\,\mu$m, $r_2 = 2.5\,\mu$m, and $r_3 = 3.6\,\mu$m for the three cases. These values are about an order of magnitude larger than the corresponding healing lengths. Note also that when decreasing the ratio between the number of particles in the vortex with respect to the vortex-free component, the actual size of the core increases, this should not be the case if we consider only the healing length.

In order to analyse the effect of increasing the vorticity upon the size of the core we set $m_2 = 2$, and verified, for example, for the second set of parameters, that the radius increased to $r_2 = 4.9\,\mu$m.

Two-dimensional model

For this mixture here we present a two-dimensional analysis and thus get rid of the variation of the vortex-core size along the z-axis. The equations derived in section 3 can be easily modified to describe this system by setting $z = d = 0$ and working with the number of particles per unit length.

To perform the numerical calculations we have chosen a number of particles which yield radii of the condensates similar to those obtained in the previous section. In figure 5 we show the GP profiles for the vorticity values $(m_1, m_2) = (0, 0), (1, 0), (0, 1)$ and $(1, 1)$. The first configuration is the ground state. For the second case, the presence of the vortex has no visible effect in the distribution of particles with respect to the ground state since the vorticity is placed in the outer species. In the third case, the vorticity of component 2 pushes the particles away from the z-axis and thus the other component fills the vortex core. It is interesting to note that although the 2-species particles do not verify $N_2 \ll N_1$, the atoms distribute themselves around the value $r' = 9.25\,\mu$m, predicted in the low-dilution regime of section 3. Finally, in

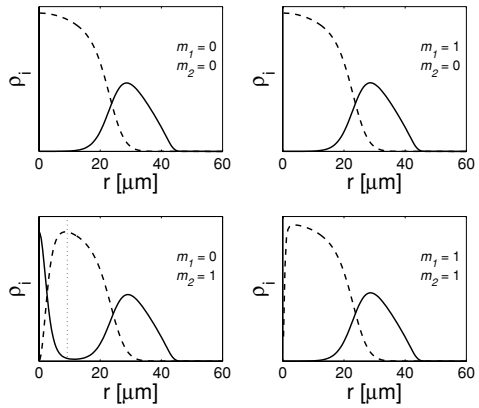

Figure 5. Density profiles (in arbitrary units) as a function of r (in units of μm) for a two-dimensional system. Each panel corresponds to different vorticity configurations (as shown in the plot). Solid and dashed lines correspond to species 1 and 2, respectively. The vertical dotted line indicates the position of r' (see the text).

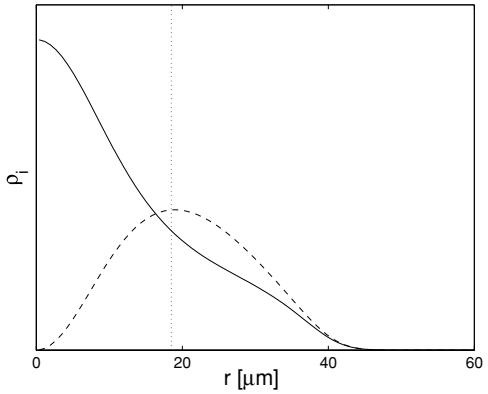

Figure 6. Density profiles (in arbitrary units) as a function of r (in units of μm) for a two-dimensional system with $(m_1, m_2) = (0, 1)$. The frequency is set to $\nu_{\rm trap} = 1.95$ Hz. Solid and dashed lines correspond to species 1 and 2, respectively. The vertical dotted line indicates the position of r' (see the text).

the last case, as both components have vorticity the distribution of components is similar to the ground state except that in this case there exists a core of the order of the healing length at the centre of the trap. For the case $(m_1, m_2) = (0, 1)$, the size of the core may be changed by varying ω_r, as we noted in section 3. In figure 6 we show a graph of the density profiles where we reduce ω_r by a factor of 4 which gives $r' = 18.5\,\mu$m. This value of r' locates rather well the maximum of the density of species 2. In addition, it may be seen in the figure that the core size is also enlarged.

5. Summary and concluding remarks

We have analysed the structure of vortices in a mixture of confined bosons and derived simple approximated expressions that well describe the spatial distribution of particles in the condensates.

On the one hand, we have obtained analytic formulae for the density profiles in the Thomas–Fermi approximation in terms of which we can easily describe the general geometrical properties of the spatial distribution of species in the condensates. By solving the Gross–Pitaevskii equations we have shown, as expected, that the TF approximation works better with an increasing number of particles. However, while in a single-component condensate this approximation is adequate for describing a system of ^{87}Rb atoms with $N \simeq 10^5$, for 2-species condensates one may need a larger number of particles, around $N \simeq 10^7$, to have a reasonable agreement with the exact solution. Two interesting and immediate results come out from these TF approximations. (i) The size of the vortex cores may be noticeably enlarged with respect to the single condensates. As a general remark, we can say that when considering vorticity in a definite component the species without vorticity fills the core, enlarging the core size sizably with respect to the corresponding one for a one-component condensate. (ii) If the minimum of the trapping potentials for each component is displaced by a distance that is small compared to the size of the total condensate, the segregation of species can change dramatically respect to the case without the displacement, effect that is also observed for the full Gross–Pitaevskii solutions.

On the other hand, we have developed some formulae for low-dilution regimes. In particular, we have obtained a simple expression for the minimum of the effective potential for 2-species particles with vorticity. Moreover, in the two-dimensional model, we have observed that this expression is adequate to locate the maximum of the density although the relation $N_2 \ll N_1$ is not satisfied.

In summary, we have derived some helpful expressions to describe the distribution of particles in two-component Bose–Einstein condensates.

Acknowledgments

This work has been partially supported by grants PID 02391 and PEI 6371 from Consejo Nacional de Investigaciones Científicas y Técnicas and EX 103 from Universidad de Buenos Aires, Argentina.

References

[1] Hall D S, Matthews M R, Wieman C E and Cornell E A 1998 *Phys. Rev. Lett.* **81** 1543
[2] Matthews M R, Anderson B P, Haljan P C, Wieman C E and Cornell E A 1999 *Phys. Rev. Lett.* **83** 2498
[3] Anderson B P, Haljan P C, Wieman C E and Cornell E A 2000 *Phys. Rev. Lett.* **85** 2857
[4] Anderson B P, Regal C A, Feder D L, Collins L A, Clark C W and Cornell E A 2001 *Phys. Rev. Lett.* **86** 2926
[5] Schweikhard V, Coddington I, Engels P, Tung S and Cornell E A 2004 *Phys. Rev. Lett.* **93** 210403
[6] Ho T-L and Shenoy V B 1996 *Phys. Rev. Lett.* **77** 3276
[7] Jezek D M, Capuzzi P and Cataldo H M 2001 *Phys. Rev.* A **64** 023605
[8] Chui S T, Ryzhov V N and Tareyeva E E 2000 *J. Exp. Theor. Phys.* **91** 1183
[9] Chui S T, Ryzhov V N and Tareyeva E E 2001 *Phys. Rev.* A **63** 023605
[10] Chui S T, Ryzhov V N and Tareyeva E E 2002 *J. Exp. Theor. Phys.* **75** 279
[11] Park Q H and Eberly J H 2004 *Phys. Rev.* A **70** 021602
[12] Jezek D M and Capuzzi P 2002 *Phys. Rev.* A **66** 015602
[13] Riboli F and Modugno M 2002 *Phys. Rev.* A **65** 063614
[14] Dalfovo F, Giorgini S, Pitaevskii L and Stringari S 1999 *Rev. Mod. Phys.* **71** 463
[15] Hall D S, Matthews M R, Ensher J R, Wieman C E and Cornell E A 1998 *Phys. Rev. Lett.* **81** 1539
[16] Press W H, Teukolsky S H, Vetterling W T and Flannery B P 1992 *Numerical Recipes in Fortran 77: The Art of Scientific Computing* (Cambridge: Cambridge University Press)
[17] Fetter A L and Svidzinsky A A 2001 *J. Phys.: Condens. Matter* **13** R135–R194